Characterization of the Continuous Elastic Parameters of Porcine Vocal Folds

[*]Garret Burks, [†]Raffaella De Vita, and [*]Alexander Leonessa, [*]*Blacksburg, Virginia, and* [†]*Blacksburg, Virginia*

Abstract: This paper presents an evaluation of the elastic properties of porcine vocal folds through uniaxial tensile tests. Inferior vocal fold tissue samples were subjected to tension in the longitudinal direction while digital image correlation techniques were employed to determine strain values throughout the tests. The stress-strain results showed a low-strain linear region, followed by both a nonlinear exponential and then a higher strain linear region. Data from 16 porcine vocal fold samples were analyzed following a similar optimization method as proposed in prior studies [1] to yield continuous model parameters which describe the elastic properties of the tissue. The average low and high strain linear modulus values were found to be 17.86 kPa and 609.27 kPa, respectively. The model also identified the location of two transition points: p_1, describing the transition from the low-strain linear region to an exponential region at 0.122 ± 0.058 mm/mm and p_2, describing the transition from the exponential to the high strain linear region at 0.308 ± 0.069 mm/mm. The exponential region of the averaged data set was found to be described by the relationship $\sigma_m(\epsilon_{xx}) = 0.083e^{19.32\epsilon_{xx}} + 2.0951$ kPa. In addition to locating transition points, the optimization method maintained modulus continuity across all strain values. Averaged elastic modulus values across strain from 0 to 0.40 mm/mm were compared to representative low and high strain linear modulus which were measured at 0.05 and 0.35 mm/mm, respectively. Statistically significant differences were found among all strain intervals between the two transition points and the linear modulus values. These results indicate the need to consider the location of transition points and further highlight the nonlinearity and changes in elastic modulus which are especially important when using excised porcine vocal folds as a model for phonation. The results quantify continuous linear and nonlinear parameters describing the elastic properties which can be used as a framework for future excised larynx tests and while evaluating the dynamics of sound production, which rely heavily on the elastic properties of the tissue.

Key Words: Vocal folds−Digital image Correlation (DIC)−Elastic modulus.

INTRODUCTION

According to the American Speech-Language-Hearing Association (ASHA), approximately 60,000 total laryngectomy patients live in the United States alone. These individuals requiring a laryngectomy, a procedure in which a patients larynx is removed often due to laryngeal cancer or severe trauma, must significantly adjust their lifestyle to compensate for their lack of vocal folds. In addition to laryngectomy patients, ASHA estimates that another 7.5 million individuals in the United States suffer from other voice-related disorders often as a result of damage to the vocal folds or surrounding tissue. The movement and control of the vocal folds within the laryngeal cavity allows for three vital functions: (1) Enabling respiration and breathing by opening the vocal folds, (2) Regulating sound production and vocalization and (3) Aiding in airway protection and enabling individuals to swallow. Due to the importance of the vocal fold tissue in numerous physiological processes and in an effort to try and improve treatment options for voice-related disorders, there have been considerable research efforts to better understand vocal fold tissue properties, vocal fold anatomy and physiology, and vocal fold dynamics during speech production. In particular, understanding tissue elasticity is crucial when studying the oscillatory behavior of the vocal folds during phonation. Due to their relative ease of availability over human cadaveric tissue, prior studies have utilized canine and porcine larynges in fully excised larynx studies while evaluating the dynamics and studying vocal fold fundamental frequencies during speech production.[2−4] While some prior studies have also been conducted to quantify tissue geometry and collect data for canine, porcine, cadaveric, and other species' vocal fold tissue elasticity, these studies have often either contained small sample sizes (≤ 6) or focused on reporting low strain secant modulus values.[5−7]

In early studies [8] of vocal fold anatomy and physiology, a cover-body division was proposed to describe human vocal folds, as illustrated in Figure 1. Additional studies[9] were conducted which further evaluated the composition of the cover layer and classified the superficial, intermediate, and deep layers in vocal fold tissue. Hahn et al presented findings in earlier studies[10,11] which highlight interspecies similarities and differences in extracellular matrix composition. Based on those reported findings,[10,11] Figure 1B illustrates the location of the superficial, intermediate, and deep layers of porcine vocal folds in comparison to human vocal folds. Notably, the porcine vocal folds have a wider superficial

Accepted for publication September 11, 2018.
Funding: This material is based upon work supported by the National Science Foundation under Grant No. 1836333.
From the Center for Dynamic Systems Modeling and Control, Department of Mechanical Engineering, Virginia Polytechnic Institute and State University, Blacksburg, Virginia; and the STRETCH Lab, Department of Biomedical Engineering and Mechanics, Virginia Polytechnic Institute and State University, Blacksburg, Virginia.
Address correspondence and reprint requests to Garret Burks, Center for Dynamic Systems Modeling and Control, Department of Mechanical Engineering, Virginia Polytechnic Institute and State University, 230 Goodwin Hall 635 Prices Fork Road, Blacksburg, VA. E-mail: garretb7@vt.edu, devita@vt.edu, aleoness@vt.edu
Journal of Voice, Vol. ■■, No. ■■, pp. 1−8
0892-1997

https://doi.org/10.1016/j.jvoice.2018.09.007

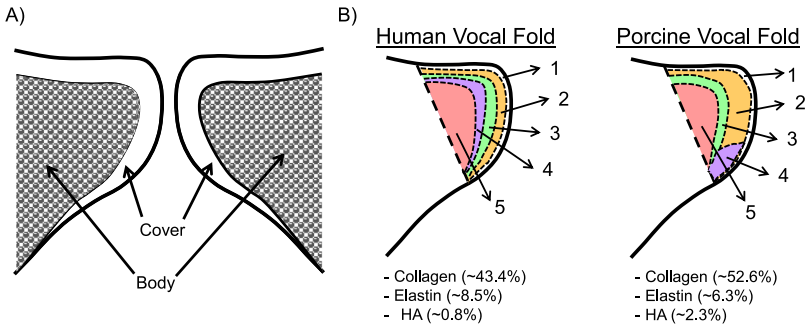

FIGURE 1. (A) Vocal fold coronal cross section illustrating cover body theory;[8,14] (B) Numbers 1−5 represent the following tissue layers in order from lowest to highest based on the findings in:[10,11] epithelium, superficial layer, intermediate layer, deep layer, muscle. The cover layer composition of human and porcine vocal folds is represented by the volume fractions of collagen, elastin, and hyaluronic acid (HA).[10−12]

layer and more inferior deep layer in comparison to human vocal folds. In addition, Figure 1 shows a comparison of extracellular matrix volume fractions in human and porcine vocal fold cover layers based on the results reported in the same study.[10−12] Other authors[13] also studied and compared the anatomy and composition of sheep, dog, pig, and human vocal folds. Through their work, the authors determined that the density of collagen and elastin fibers found in the in porcine vocal folds was most similar to that of human vocal folds.[13] These studies also highlighted that the fibers were oriented in the longitudinal direction for each of the species tested.

A variety of techniques have been used in previous studies to quantify the mechanical properties of the vocal fold tissue. In a prior study,[5] the authors measured the elastic properties of canine vocal fold tissue through uniaxial traction testing. The results of their tests showed that the stress-strain behavior of canine vocal folds exhibited linear behavior at low strains and nonlinear behavior at higher strain values. The authors reported a low strain (< 15%) secant modulus of 42 kPa and used a third-order polynomial to describe the higher strain nonlinear behavior for the canine vocal fold cover layer.[5] Other authors[6] presented results which built on this work by studying the elastic behavior of sheep, cow, and porcine vocal folds and compared them to the stress-strain results of the canine vocal folds. These tests were conducted using a similar experimental protocol as the study mentioned previously[5] and subjected the samples to approximately 40% elongation while measuring the displacement of a Dual-Servo ergometer. The initial marked length of the vocal fold samples was used to determine strain values. Similar to the results of the canine vocal fold study,[5] the authors[6] reported an average low strain (< 15%) secant modulus for the linear region of the stress-strain data for each species. The results of the interspecies study[6] indicated that the porcine vocal folds exhibited greater nonlinearity in higher strains than the other species that were tested, but the parameters describing the nonlinear behavior were not defined. The authors suggested that the greater nonlinear behavior could be an attribute of the porcine vocal folds that yield wider ranges of oscillation frequencies and make porcine samples a more suitable model for phonation. In another study,[15] researchers presented results of uniaxial traction tests on a single cadaveric vocal fold sample while using Digital Image Correlation (DIC) techniques to determine the spatial deformation field for the entire sample. The authors in this study highlighted variations in the anterior-posterior direction and found the elastic modulus to be an order of magnitude larger at the midpoint of the human vocal fold than toward the thyroid and arytenoid cartilaginous attachment points.[15]

In addition to performing uniaxial traction tests, some tests have been conducted using pig, cow, sheep, or canine fully excised larynges to further study the dynamics of phonation.[2−4,16] In one prior study,[2] researchers used DIC techniques to study the kinematics of porcine vocal folds during self-oscillation and reported on the contact stresses and strain values that were observed. Other authors have investigated biomechanical models used to predict the fundamental frequencies of speech production based on vocal fold tissue properties, such as the elastic modulus, tissue density, and in situ length of the tissue.[17−19] These models highlight the importance of the nonlinear modulus behavior on frequency changes during sound production. Due to the impact of the changing vocal fold elastic modulus on the oscillatory behavior exhibited during sound production, there is need for additional work to quantify elastic parameters at all strain values and to more accurately identify the location of transition points between the low strain linear region and higher strain modulus values.

The work detailed in this paper will highlight the results of testing 16 porcine vocal fold samples while using DIC techniques to determine strain values and collect a more complete set of tissue elasticity data during uniaxial tensile tests. Using an optimized linear-exponential model, transition points between linear and exponential regimes were determined as well as the nonlinear parameters for those regions while maintaining continuity in both the modeled stress-strain curves and resulting modulus. The continuous modulus functions can be used in future work when

evaluating the effect of changes in porcine vocal fold tissue strain and modulus on the fundamental frequencies observed during excised larynx testing.

METHODOLOGY

The following section outlines the steps used to prepare the tissue samples as well as the experimental testing methods used on the porcine vocal fold samples ($n = 16$).

Sample preparation

Sample preparation was conducted by following similar procedure to Alipour et al as described in prior studies.[5,6] Porcine larynges were obtained from adult swine through an on-campus abattoir in the Virginia Tech Department of Animal and Poultry Sciences and transported to the laboratory while immersed in a phosphate-buffered saline (PBS, pH 7.4, Fisher Scientific, USA) solution. A 2×2 inch sterile gauze pad was folded in half and placed between the left and right vocal folds while the excised larynges were submerged in a PBS solution which saturated the gauze to prevent tissue dehydration. The use of saturated gauze has been previously used as a method of tissue storage in prior studies[20] and is assumed to mitigate the adverse effects of crystallization and cracking during freezing. Each of the larynx samples was then frozen in its own container. The samples were stored at a temperature of -20 °C for a maximum duration of 6 weeks prior to testing. On the day of the experiment, the excised larynges were thawed at room temperature before removing and discarding connective tissue surrounding the thyroid cartilage as well as the epiglottis. The porcine larynx was then divided into two hemilarynges by making careful incisions from the superior region of the arytenoid cartilage down to the tracheal rings and similarly through the midline of the thyroid cartilage as shown in Figure 2. Great care was taken during incisions to avoid damage to the vocal fold tissue through punctures or excessive loading of the tissue.

After identifying the cartilaginous attachment points, incisions were made through the thyroid cartilage around the anterior attachment points of the inferior vocal folds and around the posterior attachment point through the arytenoid process. Incisions were made laterally along edges of the inferior vocal folds in order to separate the folds from surrounding tissue. After extricating the sample, extraneous muscle fibers were carefully removed from the folds. The width, length, thickness, and mass were measured using a digital caliper (accuracy ± 0.05 mm, Mitutoyo Absolute Low Force Calipers Series 573, Japan) and scale and recorded for each sample. A total of 5 measurements for both the width and thickness were collected and were used to compute an average cross-sectional area for each sample. The in situ length was measured by identifying and marking the arytenoid and thyroid cartilaginous attachment points before removing the IVF sample.

In previous studies, the inferior porcine vocal folds have been described as the true vocal folds while the superior folds were described as the ventricular folds.[13] However, more recent excised larynx tests using porcine larynges indicate that both the inferior and superior folds vibrate during phonation.[3] Due to the new information regarding the function of each vocal fold, other authors[6] have questioned the use of the labels ”true” and ”false” vocal folds for porcine larynges. Because of the lack of consensus on the use of the ”true” and ”false” labels, the authors chose to use the nomenclature ”inferior” and ”superior” which describe the vocal folds anatomical position rather than their function.

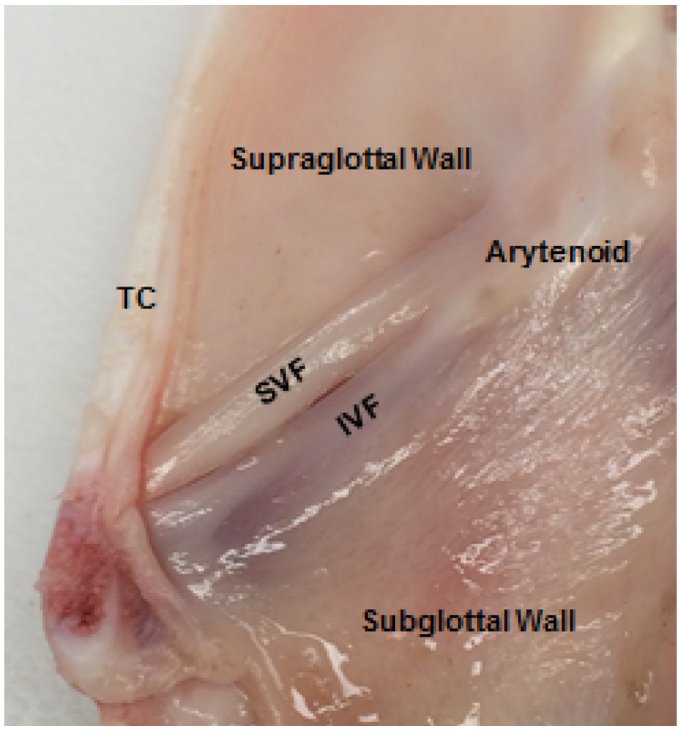

FIGURE 2. Porcine hemilarynx sample showing the arytenoid and thyroid cartilage (TC), the inferior vocal fold (IVF), superior vocal fold (SVF), subglottal wall, and supraglottal wall.

Experimental methods

After recording the sample measurements, the IVF samples were submerged for 5 minutes in a solution of PBS and methylene blue, 1% aqueous solution (Fisher Science Education, USA) following methods described by Lionello et al.[21] After 5 minutes, the samples were removed and speckled using a using an aerosol fast dry gloss white paint (McMaster-Carr, USA). Sand paper strips with a 200 grit were then cut approximately 1 cm in length and 5 mm in width and folded over the cartilaginous ends. The dyed and speckled samples were then clamped over the folded sandpaper and secured on the experimental setup as shown in Figure 3. Custom L-shaped clamps were 3D printed using a PLA plastic that were $30 \times 24 \times 20$ mm in height, width and depth, respectively, and were used to mechanically tighten the grip on the folded sandpaper over the cartilaginous ends.

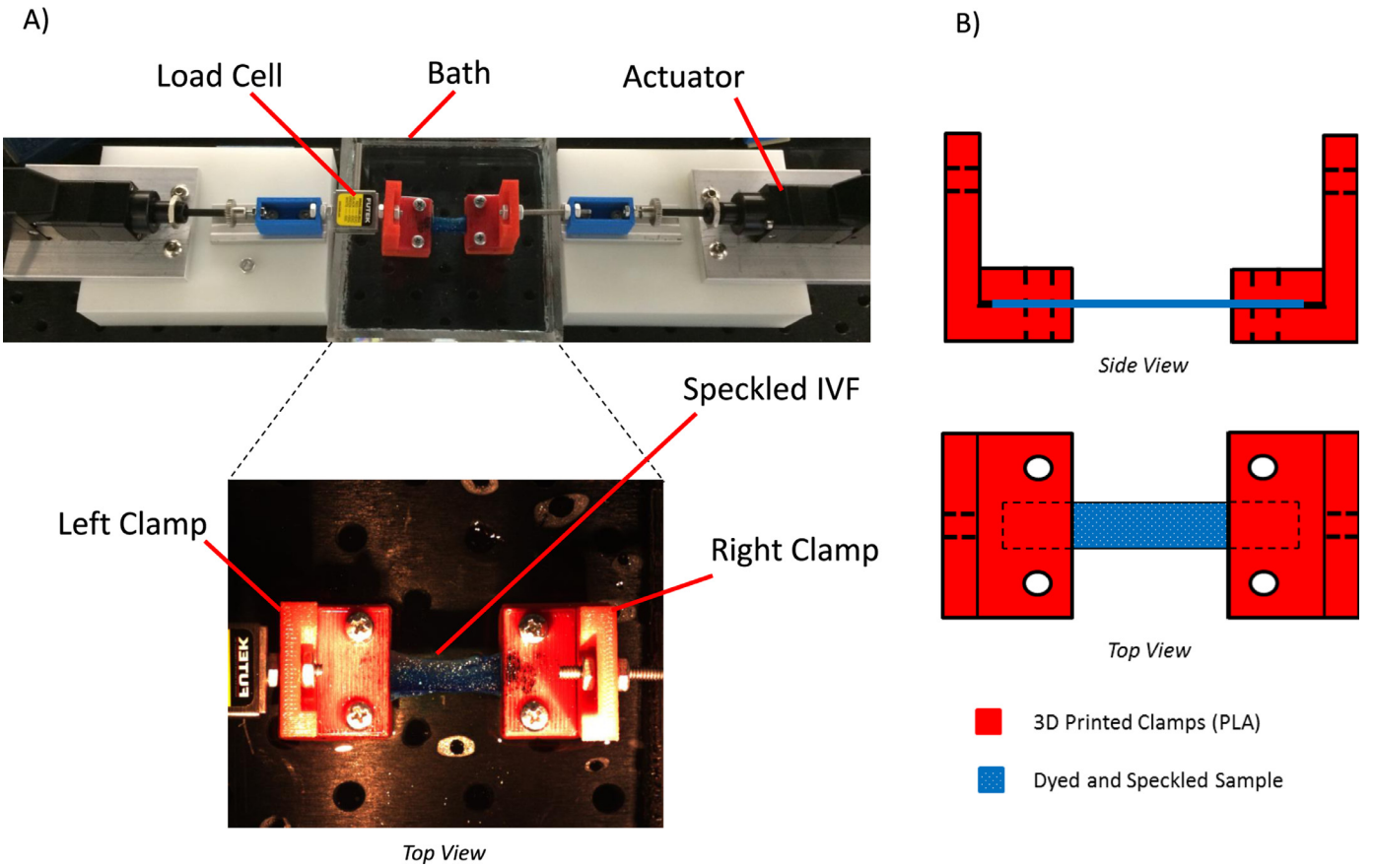

FIGURE 3. (A) Picture of the dyed and speckled sample clamped in the experimental setup. (B) Schematic of the clamps used to secure the IVF sample.

In addition, the clamps were secured to both a microscale linear actuator (Zaber T-NA) which was used to control displacement rates and a load cell (accuracy of 0.002 N, Omega 2 lbf) used to record force measurements during testing and were centrally placed in a custom built $3 \times 10 \times 10$ cm bath made of polycarbonate which allowed the sample to be submerged in a PBS solution during testing.

While securing the clamped sample to the load cell and actuator, effort was made to position the sample in the center of the field of view of a camera (Thorlabs Inc., DCC1645C) that was placed directly above the testing setup. Displacement controlled tests were conducted using the microscale linear actuator, which operated at a displacement rate of 0.033 mm/s during all tension tests. The load cell was then zeroed after obtaining a desired preload of 0.02 N. Displacement controlled tensile tests were performed while stretching the sample to approximately 40% strain (displacement was limited by maximum actuator stroke distance) while recorded images of 1280×1024 pixels were taken at a rate of 4 Hz with a field of view of 8.0×8.0 cm. Actuator position, force, and video data were recorded synchronously to a desktop computer via a data acquisition module (National Instruments NI cDAQ-9172) using LabVIEW (National Instruments).

All stress and strain values were calculated referenced from the preloaded configuration. Engineering strain of the IVF sample was calculated using DIC methods implemented in MATLAB.[22] Previous studies have demonstrated the successful implementation of this noncontact strain measurement method in biological materials.[23] For each of our samples, we chose to compute strain values based on a rectangular grid of 25 points in the center region of the IVF sample. The engineering strain was then found by taking the average of the engineering strain values computed from each of the 25 points. The nominal stress, σ, was calculated using the following relationship

$$\sigma = \frac{F}{wt}, \tag{1}$$

where F, is the measured tensile force, and w and t are the average width and thickness, respectively, of the IVF sample.

Model optimization

The calculated stress and strain values were then analyzed through a combination of optimized linear and exponential continuous functions. The continuous model was based on the methodology presented by Tanaka et al[1] in a previous study, which highlighted its benefits over using conventional curve-fitting techniques when

computing linear and exponential parameters for soft biological materials. As pointed out in the prior study, efforts to model soft biological data using traditional piecewise methods often lead to discontinuities between the linear and exponential regions or result in a discontinuous modulus. The continuous method by Tanaka[1] minimizes the mean square error (MSE) while simultaneously calculating the linear parameters, exponential parameters, and the location of a transition point between the two regions. Our model employed a similar method to determine the location of a transition point between a low strain linear region and an exponential region as well as a secondary transition point between the exponential region and a high strain linear region. The model minimized both the MSE and the percent error while calculating all linear and exponential parameters as well as the location of the two transition points.

The following equations describe the continuous model

$$\sigma_{\mathrm{m}}(\epsilon_{xx}) = \begin{cases} m_1\epsilon_{xx}, & \epsilon_{xx} < p_1, \\ ae^{b\epsilon_{xx}} + q_1, & p_1 \le \epsilon_{xx} < p_2, \\ m_2\epsilon_{xx} + q_2, & p_2 \le \epsilon_{xx}, \end{cases} \tag{2}$$

where σ_{m} is the model calculated stress, ϵ_{xx} is the engineering strain in the longitudinal direction, and (p_1, q_1) and (p_2, q_2) are transition points between the linear and exponential regions of the stress-strain data. In addition, m_1, m_2 and *a, b*, are model parameters of the linear and exponential regions, respectively. In order to ensure continuity at the transition points, the slopes of the linear regions m_1 and m_2, and the stress values at the transition points, q_1 and q_2 are defined in terms of *a* and *b* using the following relationships,

$$m_1 = abe^{b\epsilon_{xx}(p_1)}, \tag{3}$$

$$m_2 = abe^{b\epsilon_{xx}(p_2)}, \tag{4}$$

$$q_1 = ab\epsilon_{xx}(p_1)e^{b\epsilon_{xx}(p_1)} \tag{5}$$

$$q_2 = ae^{b\epsilon_{xx}(p_2)} + q_1. \tag{6}$$

The continuous model utilized the MATLAB® function *fmincon* to calculate parameters *a, b,* p_1 and p_2 while minimizing the MSE and percent error which were defined by

$$\mathrm{MSE} = \frac{1}{n}\sum_{i=1}^{n}\left(\sigma_{\mathrm{m}}(i) - \sigma(i)\right)^2, \tag{7}$$

$$\%\mathrm{Error(i)} = \frac{\sigma(i) - \sigma_{\mathrm{m}}(i)}{\sigma(i)}, \tag{8}$$

where *i* is the index number that corresponds to each data point and *n* is the total number of data points being analyzed. Figure 4 illustrates the continuous model fit to data collected from a representative sample.

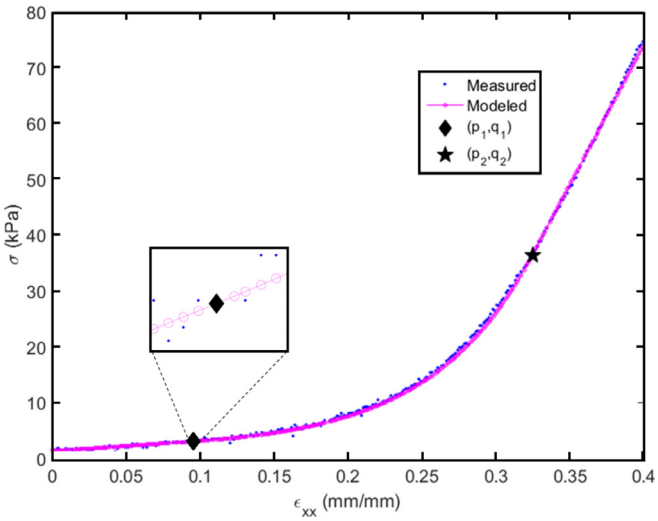

FIGURE 4. Continuous model analyzed for porcine IVF sample.

Statistical analysis

Elastic model parameters were determined for each of the 16 samples using the continuous optimization method described previously. Modulus values were recorded for each sample from 0 to 0.40 mm/mm strain at an interval of 0.05 mm/mm. A student's *t* test was then used to compare the modulus values at various strain values to an average low strain modulus (mean modulus at 0.05 mm/mm) and a high strain modulus (0.35 mm/mm). The threshold chosen for statistical significance was 0.05. Data were analyzed using the JMP statistical software (JMP, Version 10, SAS Institute Inc.).

RESULTS

The average recorded length, width, and thickness for the porcine vocal fold samples was found to be 25.69 ± 4.8 mm, 5.57 ± 1.31 mm, and 1.91 ± 0.62 mm, respectively. Data from each of the 16 IVF samples was analyzed individually to obtain model parameters. Analyzing the sample data individually enabled the calculation of standard deviation values for the transition points, which can be found in Table 1. Figure 5 displays the average stress, σ_{mean}, for the total data set of all 16 porcine IVF tension tests along with the shaded regions representing ± standard deviation across all strain values for the samples tested. Results of all linear and exponential parameters calculated

TABLE 1.
Mean and Standard Deviation Model Parameter Values

	m_1	*a*	*b*	m_2	p_1	p_2
σ_{mean}	17.86	0.083	19.32	609.27	0.122	0.308
STD	7.91	-	-	236.73	0.058	0.069

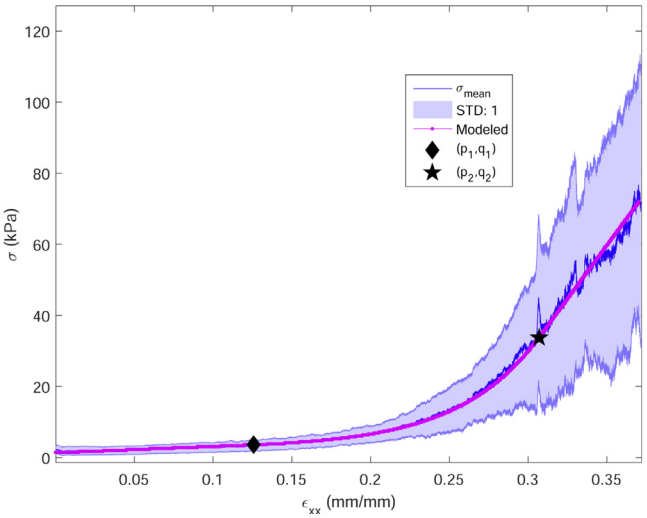

FIGURE 5. Mean and standard deviation of stress-strain data collected from 16 IVF porcine samples (parameters for continuous model can be found in Table 1).

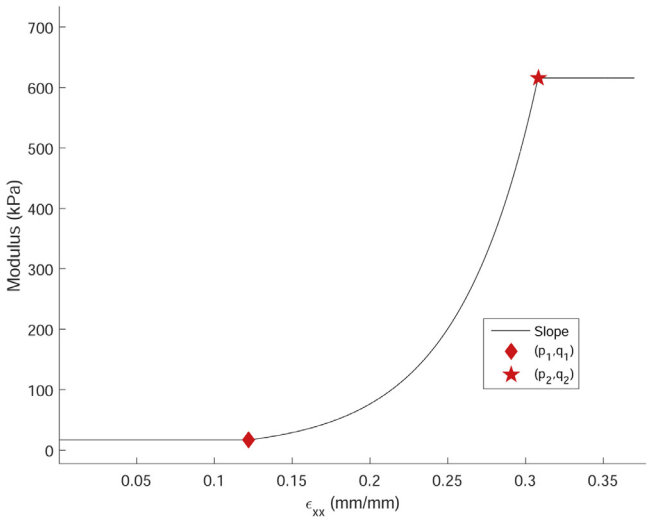

FIGURE 6. Continuous model modulus highlighting transition points and linear and exponential regions.

from the continuous model can be seen in Table 1. The slope of the low-strain linear region ($\epsilon_{xx} < p_1$) was found to be 17.86 ± 7.91 kPa while the slope in the high-strain region ($\epsilon_{xx} > p_2$) was 609.27 ± 236.73 kPa. The transition points p_1 and p_2 were found to be 0.122 ± 0.058 and 0.308 ± 0.069 mm/mm, respectively. The standard deviation for the transition points were calculated by evaluating the values of p_1 and p_2 for each of the 16 IVF samples. The parameters a and b were determined from the averaged data set to describe the nonlinear region between transition points p_1 and p_2 and can be found in Table 1. The exponential equation, $\sigma_m(\epsilon_{xx}) = 0.083e^{19.32\epsilon_{xx}} + 2.0951$ kPa, follows the form of $\sigma_m(\epsilon_{xx}) = ae^{b\epsilon_{xx}} + q_1$ to describe the stress-strain relationship between the transition points where $q_1 = \sigma(p_1)$.

The elastic modulus, E, was calculated from the continuous model, where $E = \frac{d\sigma_m}{d\epsilon_{xx}}$. The resulting modulus can be seen in Figure 6 plotted with respect to the strain. As described previously, the continuous model maintains continuity throughout the transitions points. The modulus of low and high strain linear regions can be represented by the constants m_1 and m_2, while the nonlinear region, which is evaluated at strain values, ϵ_{xx}, between p_1 and p_2, can be described by $abe^{b\epsilon_{xx}}$ where a and b are constants as shown in Table 1.

Modulus values were calculated for each of the tests individually and recorded at engineering strain values from 0 to 0.40 mm/mm at an interval of 0.05 mm/mm. Table 2 highlights the average modulus, E_{mean}, and standard error of the mean (SEM) values for each of the recorded strain values. A student t test was conducted to compare each set of modulus values to a low and high strain modulus value evaluated at 0.05 mm/mm and 0.35 mm/mm respectively. The resulting P values highlighting differences in the compared modulus values can be see in Table 2. A comparison between the low-strain modulus value evaluated at 0.05 mm/mm and recorded values at 0.10 mm/mm showed no statistically significant differences ($P = 0.173$). All other strain intervals greater than 0.10 mm/mm, however, indicated significant differences ($P < 0.05$) from the recorded values at 0.05 mm/mm. Conversely, all strain intervals lower than 0.30 mm/mm were found to have significant differences when compared to the recorded high strain modulus values at 0.35 mm/mm. These results are found to be in agreement with the location of the transition points, where all of the strain intervals between p_1 and p_2 have statistically significant differences when compared to the low and high strain linear modulus values.

DISCUSSION

The average low-strain modulus was compared to the results reported in a prior study[6] of porcine inferior vocal folds where a value of 16.3 ± 1.9 kPa was determined. The results in this study are found to be in agreement with no statistically significant differences (P value = 0.486) in the reported finding and a 8.73% difference in the average low-strain modulus. In addition, the modulus results were compared to prior studies which reported findings on human true vocal folds samples and prior tests of canine vocal fold cover layer samples.[5,7] At low-strains, Alipour et al[5] reported an average canine cover vocal fold modulus of 41.9 ± 7.1 kPa while a high strain modulus evaluated at 35% strain was determined to be 132 kPa based off the reported third-order polynomial. In a different study, the authors[7] determined a low-strain modulus value of 28 kPa for human vocal fold samples while a high strain modulus value was found to be 390 kPa between 30% and 35% strain. The low strain modulus for the porcine IVF was found to be lower than the reported findings for both the human vocal fold samples[7] and the canine vocal fold cover samples.[5] The porcine IVF samples, however, exhibited higher modulus

TABLE 2.
Mean and standard error of the mean modulus values for different engineering strain as well as the resulting *P* values from individual Student *t* tests to compare the modulus at each strain interval to the low and high strain modulus values of 0.05 and 0.35 mm/mm, respectively

ϵ_{xx}	0.05	0.10	0.15	0.20	0.25	0.30	0.35
E_{mean}	17.68	21.68	39.00	87.44	224.14	517.15	651.97
SEM	1.56	2.32	7.04	19.45	51.17	123.99	111.04
Low: *P*	-	**0.173**	0.011	0.002	< 0.001	< 0.001	< 0.001
High: *P*	< 0.001	< 0.001	< 0.001	< 0.001	0.003	**0.483**	-

values at higher strains than the canine or human results presented.[5,7]

As Figures 5 and 6 illustrate, the results demonstrate the nonlinear elasticity of the porcine vocal folds. The nonlinearity of the tissue is thought to be a result of collagen fiber recruitment occurring as the sample is stretched, while the low-strain linear region occurs before the collagen fibers are under tension and bear load.[24] At low strains, collagen fibers may exist in a crimped or wavy state. As the vocal folds are elongated, the collagen fibers can begin to straighten and eventually become taut and load bearing. An increasing number of collagen fibers may be recruited under tension as the tissue stretches which could contribute to the nonlinear stress-strain response. The linear low-strain modulus can be assumed to be a result of the elastin content in the tissue before the collagen recruitment occurs around the transition point p_1.

This study focused on only uniaxial elastic tensile tests of porcine inferior vocal folds, which have been previously used in excised larynx testing.[2] Although biaxial tension tests are typically preferred to characterize tissue responses to varying loads, geometric constraints requiring tissue sample sizes of at least 3×3 cm prevented these tests from occurring using the porcine vocal fold samples. Prior studies have indicated that the composition of pig vocal folds is more similar to humans than canine, cow, or sheep vocal folds and could be a particularly useful model of phonation.[10,11] The nonlinear stress-strain relationship found in porcine vocal folds could be especially helpful when evaluating frequency changes during vocal fold vibration. As indicated in previous studies,[6] porcine vocal folds may be likely strain rate dependent and the nonlinear stress-strain curves, including the elastic parameters of the proposed model, may change at different strain rates. For this reason, future experiments should be conducted to further explore the viscoelasticity of the tissue with regard to the nonlinear elastic properties.

In a prior study,[15] researchers investigated the spatially-varying elastic properties of one human vocal ligament. It is possible that porcine vocal folds also exhibit spatially varying elasticity. To our knowledge, there have not been investigations on the spatial variations in elasticity of the porcine vocal fold cover layer. The authors of the prior study,[15] also posed questions and investigated how the spatially varying elasticity would impact the eigenfrequency response of the tissue during phonation. Similarly, it would be of interest to investigate the spatial variations in porcine vocal folds and also investigate how those variations impact the dynamic response of the tissue during sound production. In addition, it is important to note that the strain values were computed in this study by tracking 25 points in center region of the tissue. Thus, spatial variations in the porcine tissue elasticity could lead to differences in the recorded strain values when using different methods to compute the tissue strain such as clamp displacement.

Non-contact means of measuring strain, such as DIC, are typically more appropriate when evaluating the tissue strain during excised larynx tests and have been used in prior studies.[2] The use of DIC methods in our study to help produce the continuous model parameters can be used as a foundation for future tests using excised porcine vocal folds to evaluate sound production. In particular, our results indicate the need to consider the location of transition points p_1 and p_2 and the corresponding change in elastic modulus between the low and high strain linear regions during excised larynx testing.

As mentioned previously, models of vocal fold vibration rely heavily on the elastic properties of the tissue.[17] When studying the vibration of vocal folds during excised larynx tests and, in particular, evaluating frequency changes produced by the tissue, it is necessary to have a clear understanding of how the modulus changes with tissue strain. Thus, the development of a comprehensive continuous modulus model that evaluates transition points between the linear and exponential regions while also employing the use of non-contact DIC methods for measuring strain values can be particularly useful in future studies to evaluate phonation dynamics using excised porcine vocal folds.

REFERENCES

1. Tanaka ML, Weisenbach CA, Miller MC, et al. A continuous method to compute model parameters for soft biological materials. *J. Biomech. Eng*. 2011;133:074502.
2. Bakhshaee H, Young J, Yang JCW, et al. Determination of strain field on the superior surface of excised larynx vocal folds using DIC. *J Voice*. 2013;27:659–667.

3. Alipour F, Jaiswal S. Phonatory characteristics of excised pig, sheep, and cow larynges. *J Acoust Soc Am*. 2008;123:4572–4581.
4. Alipour F, Jaiswal S. Glottal airflow resistance in excised pig, sheep, and cow larynges. *J Voice*. 2009;23:40–50.
5. Alipour-Haghighi F, Titze IR. Elastic models of vocal fold tissues. *J Acoust Soc Am*. 1991;90:1326–1331.
6. Alipour F, Jaiswal S, Vigmostad S. Vocal fold elasticity in the pig, sheep, and cow larynges. *J Voice*. 2011;25:130–136.
7. Alipour F, Vigmostad S. Measurement of vocal folds elastic properties for continuum modeling. *J Voice*. 2012;26. 816.e21−816.e29
8. Hirano M. Morphological structure of the vocal cord as a vibrator and its variations. *Folia Phoniatrica et Logopaedica*. 1974;26:89–94.
9. Hirano M, Kakita Y, Ohmaru K. Structure and mechanical properties of the vocal fold. *Speech Lang*. 1982;7:271–297.
10. Hahn MS, Kobler JB, Zeitels SM. Quantitative and comparative studies of the vocal fold extracellular matrix II: collagen. *Ann Otol Rhinol Laryngol*. 2006;115:225–232.
11. Hahn MS, Kobler JB, Starcher BC, et al. Quantitative and comparative studies of the vocal fold extracellular matrix i: elastic fibers and hyaluronic acid. *Ann Otol Rhinol Laryngol*. 2006;115:156–164.
12. Miri AK. Mechanical characterization of vocal fold tissue: a review study. *J Voice*. 2014;28:657–667.
13. Kurita S. A comparative study of the layer structure of the vocal fold. *Vocal Fold Phsiology: contemporary research and clinical issues* 1983;3–21.
14. Story BH. An overview of the physiology, physics and modeling of the sound source for vowels. *Acoust Sci Technol*. 2002;23:195–206.
15. Kelleher JE, Zhang K, Siegmund T, et al. Spatially varying properties of the vocal ligament contribute to its eigenfrequency response. *J Mech Behav Biomed Mater*. 2010;3:600–609.
16. Alipour F, Scherer RC, Finnegan E. Pressure-flow relationships during phonation as a function of adduction. *J Voice*. 1997;11:187–194.
17. Zhang K, Siegmund T, Chan RW, et al. Predictions of fundamental frequency changes during phonation based on a biomechanical model of the vocal fold lamina propria. *J Voice*. 2009;23:277–282.
18. Zhang K, Siegmund T, Chan RW. A two-layer composite model of the vocal fold lamina propria for fundamental frequency regulation. *J Acoust Soc Am*. 2007;122:1090–1101.
19. Zhang K, Siegmund T, Chan RW. A constitutive model of the human vocal fold cover for fundamental frequency regulation. *J Acoust Soc Am*. 2006;119:1050–1062.
20. Lee AH, Elliott DM. Freezing does not alter multiscale tendon mechanics and damage mechanisms in tension. *Ann NY Acad Sci*. 2017;1409:85–94.
21. Lionello G, Sirieix C, Baleani M. An effective procedure to create a speckle pattern on biological soft tissue for digital image correlation measurements. *J Mech Behav Biomed Mater*. 2014;39:1–8.
22. Eberl C., Thompson R., Gianola D.. Digital image correlation and tracking with matlab, matlab file exchange. 2006.
23. Zhang D, Arola DD. Applications of digital image correlation to biological tissues. *J Biomed Opt*. 2004;9:691–699.
24. Humphrey JD. *Cardiovascular Solid Mechanics: Cells, Tissues, and Organs*. Springer Science & Business Media; 2013.